Microscopic insights into the London penetration depth: Application to $CeCoIn_5$

Mehdi Biderang [1], Jeehoon Kim,[2] Reza Molavi,[3,4] and Alireza Akbari [5,6]

[1]*Department of Physics, University of Toronto, 60 St. George Street, Toronto, Ontario, Canada M5S 1A7*
[2]*Department of Physics, POSTECH, Pohang, Gyeongbuk 790-784, Korea*
[3]*Department of Electrical and Computer Engineering, University of British Columbia, Vancouver, British Columbia, Canada V6T 1Z4*
[4]*D-Wave Systems Incorporated, Burnaby, British Columbia, Canada V5G 4M9*
[5]*Institut für Theoretische Physik III, Ruhr-Universität Bochum, D-44801 Bochum, Germany*
[6]*Asia Pacific Center for Theoretical Physics (APCTP), Pohang, Gyeongbuk 790-784, Korea*

(Received 30 September 2023; revised 9 November 2023; accepted 21 December 2023; published 16 January 2024)

We propose a comprehensive theoretical formulation of the magnetic penetration depth $\lambda(T)$ based on microscopic calculations for a general superconducting gap symmetry. Our findings admit the significant role of band structure and Fermi-surface topology together with the symmetry of the superconducting order parameter. We employ our findings pertaining to the heavy-fermion superconductor $CeCoIn_5$ to explore both local (London) and nonlocal (Pippard) behaviors in response to an external magnetic field across varying temperatures. Our calculations in the low-temperature regime offer compelling macroscopic evidence of the nodal character within the superconducting state with $d_{x^2-y^2}$ symmetry. Furthermore, our findings align with the characteristics of Pippard-type superconductivity, holding significant implications for upcoming experiments.

DOI: 10.1103/PhysRevB.109.014512

I. INTRODUCTION

The discovery of unconventional superconductivity has opened up exciting avenues of research, offering unprecedented insights into the fundamental properties of matter [1–3]. The superconducting properties have been extensively investigated using various theoretical and experimental techniques, shedding light on its electronic structure, pairing mechanism, and gap symmetry [4,5]. Of particular significance is the measurement of the London penetration depth, a fundamental property that delineates a superconductor's response to an applied magnetic field [6–11]. The experimental studies employing diverse techniques, such as muon spin rotation (μSR), specific heat measurements, scanning tunneling microscopy (STM), and magnetic force microscopy (MFM), have explored the penetration depth [12–18]. To illustrate the significance of the London penetration depth in practical applications, it is worthwhile to recognize that superconducting quantum bits (qubits) are typically designed to possess specific body inductance comprising two major components, geometric and kinetic inductance. The latter term is heavily impacted by the London penetration depth, further underscoring the necessity of its accurate modeling to predict individual qubit performance in a large-scale quantum processor [19]. The temperature-dependent behavior of the penetration depth and related superfluid density provides direct windows into the nature of the superconducting gap [20–22]. These investigations have revealed intriguing behavior, including a rapid suppression of the superfluid density with increasing temperature, unconventional power-law temperature dependencies, and the presence of nodes or anisotropic gap structures in the superconducting state [23–26]. Consequently, it becomes a reflection of the interplay between the superconducting gap structure and the topology of the Fermi surface [27,28]. A comprehensive understanding of the penetration depth in both "specular" and "diffuse" regimes is crucial for investigating the designing devices that utilize superconductors, such as high-speed electronics, magnetic resonance imaging (MRI) machines, or particle accelerators.

Heavy-fermion compounds have risen as captivating systems that manifest unconventional superconductivity, pushing the boundaries of our comprehension beyond the confines of the conventional Bardeen-Cooper-Schrieffer (BCS) theory [29–31]. Among these compounds, $CeCoIn_5$ has attracted considerable attention due to its intriguing superconducting properties and the presence of a complex superconducting gap structure [32–37]. It is a unique heavy-fermion compound that crystallizes in a tetragonal $HoCoGa_5$-type structure and exhibits superconductivity below a critical temperature of $T_c \approx 2.3$ K [32]. This compound is of particular interest because it resides in close proximity to a quantum critical point, where tiny perturbations can induce significant changes in its electronic properties. This proximity to a quantum critical point hints at the possibility of unconventional Cooper pairing, emphasizing the intricate interplay between magnetism and superconductivity [38,39]. These findings challenge conventional models and highlight the need for a comprehensive study to elucidate the superconducting gap function. Several hypotheses regarding its superconducting gap function have been explored, drawing from thermodynamic and transport properties. The evidence suggests a spin singlet gap with d-wave pairing. Initially, conflicting results hinted at both $d_{x^2-y^2}$ and d_{xy} gap symmetries [33,40]. However, a distinct spin resonance observed via inelastic neutron scattering strongly supports the $d_{x^2-y^2}$ symmetry [41–43]. Additionally, low-temperature field-angle-resolved specific heat measurements provided further confirmation of this symmetry [44], and subsequent quasiparticle interference (QPI) measurements reinforced it [45–47].

In addition to providing strong evidence for the d-wave properties of $CeCoIn_5$, the most recent magnetic force microscopy results have shown a peculiar power-law pattern in the penetration depth [48]. Inspired by these discoveries, our work presents a comprehensive theoretical analysis of the penetration depth in such materials, utilizing microscopic approaches. We take into account both local and nonlocal responses as we investigate the behavior of penetration depth across a broad temperature range. Our primary goal is to give a thorough explanation of its dependence on the superconducting gap symmetry. In this regard, Sec. II outlines the physical model used to describe the electronic band structure. In Sec. III, we introduce the response of a superconductor to an external electromagnetic field and establish a microscopic model to investigate the magnetic penetration depth within a superconducting context. Lastly, in Sec. IV, we consolidate our findings, presenting potential scenarios for the superconducting gap function in $CeCoIn_5$.

II. MODEL HAMILTONIAN OF A HEAVY-FERMION SYSTEM

The Anderson lattice model Hamiltonian, which takes into account the hybridization between the doubly spin-degenerate conduction and localized orbitals, can be represented as [49]

$$\mathcal{H} = \mathcal{H}_0 + \mathcal{H}_{\text{int}}, \tag{1}$$

with the noninteracting part of the Hamiltonian represented by

$$\mathcal{H}_0 = \sum_{\mathbf{k},\sigma} \varepsilon^c_{\mathbf{k}} c^\dagger_{\mathbf{k},\sigma} c_{\mathbf{k},\sigma} + \varepsilon^f_{\mathbf{k}} f^\dagger_{\mathbf{k},\sigma} f_{\mathbf{k},\sigma} + \frac{1}{2}(V_{\mathbf{k}} c^\dagger_{\mathbf{k},\sigma} f_{\mathbf{k},\sigma} + \text{H.c.}), \tag{2}$$

and the on-site Coulomb interaction among the f electrons given by

$$\mathcal{H}_{\text{int}} = \sum_{\mathbf{k}\mathbf{k}'} U_{ff} f^\dagger_{\mathbf{k},\uparrow} f_{\mathbf{k},\downarrow} f^\dagger_{\mathbf{k}',\uparrow} f_{\mathbf{k}',\downarrow}. \tag{3}$$

Here, the creation of a conduction (localized) electron of momentum $\mathbf{k}$ and spin σ is denoted by $c^\dagger_{\mathbf{k},\sigma}$ ($f^\dagger_{\mathbf{k},\sigma}$). The hybridization between the lowest $4f$ doublet and conduction bands occurs through $V_{\mathbf{k}}$, encompassing the influence of spin-orbit coupling and crystal field effects. As the on-site Coulomb interaction U_{ff} tends towards an extremely large value, the existence of doubly occupied f states becomes energetically forbidden. Consequently, by introducing auxiliary bosons, the mean-field (MF) Hamiltonian of the quasiparticle bands can be expressed as follows,

$$\mathcal{H}_{\text{MF}} = \sum_{\mathbf{k},s,\sigma} \xi_{\mathbf{k},s} a^\dagger_{\mathbf{k},s,\sigma} a_{\mathbf{k},s,\sigma}, \tag{4}$$

where $a^\dagger_{\mathbf{k},s,\sigma}$ is an operator of creation of a quasiparticle at band $s = \pm$ and spin σ. The dispersion of quasiparticles is given by

$$\xi_{\mathbf{k},\pm} = \tfrac{1}{2}\left[\varepsilon^c_{\mathbf{k}} + \varepsilon^f_{\mathbf{k}} \pm \sqrt{\left(\varepsilon^c_{\mathbf{k}} - \varepsilon^f_{\mathbf{k}}\right)^2 + V^2_{\mathbf{k}}}\right]. \tag{5}$$

The effective hybridization between conduction and localized electrons is denoted by $\tilde{V}_{\mathbf{k}} = V_{\mathbf{k}}\sqrt{1 - n_f}$, where n_f represents the occupancy of the localized electron states and ensures the exclusion of double occupancy. Extensive studies have demonstrated that the formation of the Fermi surface is solely attributed to the $s = -$ band, while the $s = +$ band resides above the Fermi energy. This phenomenon becomes evident in a three-dimensional arrangement within a tetragonal crystal lattice, with a distinct emphasis on the C_{4v} rotational symmetry within the xy plane. By employing the model detailed in Refs. [45,49], we illustrates the Fermi surface of $CeCoIn_5$ in Fig. 1. Moreover, the superconducting state of the system can be described by

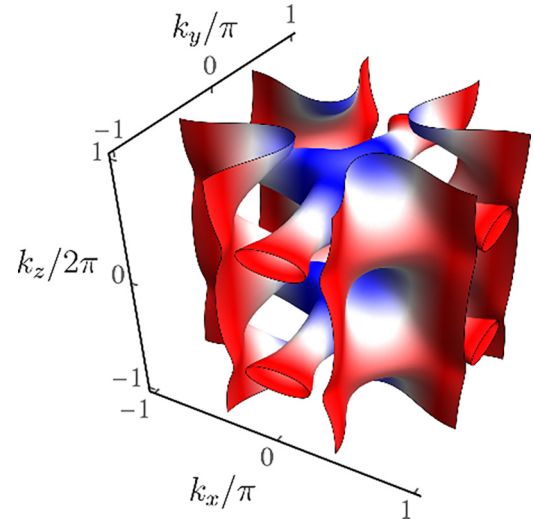

FIG. 1. Calculated three-dimensional Fermi surfaces of $CeCoIn_5$ based on the Anderson lattice model.

$$\mathcal{H}_{\text{SC}} = \sum_{\mathbf{k},s} (\Delta_{\mathbf{k}} a^\dagger_{\mathbf{k},s,\uparrow} a^\dagger_{-\mathbf{k},s,\downarrow} + \text{H.c.}), \tag{6}$$

wherein $\Delta_{\mathbf{k}}$ represents the superconducting gap function in the singlet channel. Extensive research has established that the gap function symmetry in $CeCoIn_5$ exhibits the characteristic nodal structure of d-wave pairing.

III. RESPONSE OF A SUPERCONDUCTOR IN A WEAK ELECTROMAGNETIC FIELD

We investigate the response of a superconductor to an external weak electromagnetic field, which is significantly smaller than the critical magnetic fields. We focus our analysis on a semi-infinite three-dimensional $CeCoIn_5$ superconductor with a planar surface located at $z = 0$, occupying the half space ($z < 0$). This system is exposed to a constant weak magnetic field (Meissner state) in the y direction. The current density $\mathbf{J}$ is connected to the vector potential $\mathbf{A}$ through the relation [7]

$$\mathbf{J}(\mathbf{r}, t, T) = -\int \mathbb{K}(\mathbf{r} - \mathbf{r}', t - t', T)\mathbf{A}(\mathbf{r}', t')d\mathbf{r}'dt', \tag{7}$$

where $\mathbb{K}$ represents the nonlocal electromagnetic response kernel. In the microscopic theory, this quantity is expressed as the charge current–charge current correlation function at temperature T. In our formalism, we have opted to employ the following unit conventions: $\hbar, k_B, c \equiv 1$. Performing a Fourier

transformation over space and time gives the correlation function in momentum and frequency spaces as

$$\mathbf{J}(\mathbf{q},\omega,T)=-\mathbb{K}(\mathbf{q},\omega,T)\mathbf{A}(\mathbf{q},\omega). \tag{8}$$

In the context of linear response theory and through the application of the Kubo formula, this correlation function is defined as

$$\mathbb{K}_{\alpha\beta}(\mathbf{q},\omega_m,T)=\mathbb{K}_0\delta_{\alpha\beta}+\Delta\mathbb{K}_{\alpha\beta}(\mathbf{q},\mathrm{i}\omega,T)\big|_{\mathrm{i}\omega\to\omega_m+\mathrm{i}0^+}, \tag{9}$$

where $\mathbb{K}_0=ne^2/m$, and n, e, and m are the density, charge, and bare mass of the electron, respectively. It should be emphasized that $\mathbb{K}_0$ is solely a band structure property and is related to the magnetic penetration depth $\lambda(0)=\lambda_0$ at absolute zero temperature. Moreover, the temperature-dependent part of the response function determining the deviation of the magnetic penetration depth from λ_0 is given by [50]

$$\Delta\mathbb{K}_{\alpha\beta}(\mathbf{q},\mathrm{i}\omega_m,T)=-\frac{T}{4N}\sum_{\mathbf{k},\mathrm{i}\nu_n}\hat{J}^{\alpha}_{\mathbf{k}}\hat{\mathcal{G}}_{\mathbf{k}}(\mathrm{i}\nu_n)\hat{J}^{\beta}_{\mathbf{k}}\hat{\mathcal{G}}_{\mathbf{k}+\mathbf{q}}(\mathrm{i}\omega_m+\mathrm{i}\nu_n), \tag{10}$$

in which $\omega_m=2m\pi$ stands for bosonic Matsubara frequency. In addition,

$$\hat{J}^{\alpha}_{\mathbf{k}}=\begin{bmatrix}J^{\alpha,e}_{\mathbf{k}} & 0\\ 0 & J^{\alpha,h}_{\mathbf{k}}\end{bmatrix} \tag{11}$$

represents the 2×2 matrix of the αth component of the charge current in Nambu space $(a^{\dagger}_{\mathbf{k},-,\uparrow},a_{-\mathbf{k},-,\downarrow})$, whose elements are defined by [51,52]

$$J^{\alpha,e}_{\mathbf{k}}=-\frac{\partial\xi_{\mathbf{k}+e\mathbf{A}}}{\partial A_\alpha}\bigg|_{\mathbf{A}=0},\quad J^{\alpha,h}_{\mathbf{k}}=\frac{\partial\xi_{-\mathbf{k}+e\mathbf{A}}}{\partial A_\alpha}\bigg|_{\mathbf{A}=0}. \tag{12}$$

Furthermore, the Matsubara Green's function is

$$\hat{G}(\mathbf{k},\mathrm{i}\nu)=\begin{bmatrix}\mathcal{G}(\mathbf{k},\mathrm{i}\nu_n) & \mathcal{F}(\mathbf{k},\mathrm{i}\nu_n)\\ \mathcal{F}^{\dagger}(\mathbf{k},\mathrm{i}\nu_n) & -\mathcal{G}^{T}(-\mathbf{k},-\mathrm{i}\nu_n)\end{bmatrix}, \tag{13}$$

where

$$\mathcal{G}(\mathbf{k},\mathrm{i}\nu_n)=\frac{\mathrm{i}\nu_n+\xi_{\mathbf{k},-}}{(\mathrm{i}\nu_n)^2-E^2_{\mathbf{k},-}},\quad \mathcal{F}(\mathbf{k},\mathrm{i}\nu_n)=\frac{-\Delta_{\mathbf{k}}}{(\mathrm{i}\nu_n)^2-E^2_{\mathbf{k},-}} \tag{14}$$

are normal and anomalous Green's functions, respectively, with the fermionic Matsubara frequency $\nu_n=(2n+1)\pi T$ at finite temperature T, and the quasiparticle dispersion $E_{\mathbf{k},-}=\sqrt{\xi^2_{\mathbf{k},-}+\Delta^2_{\mathbf{k}}}$. Thus in the superconducting state, $\Delta\mathbb{K}_{\alpha\beta}(\mathbf{q},\omega,T)$ can be simplified as

$$\Delta\mathbb{K}_{\alpha\beta}(\mathbf{q},\omega,T)=\frac{1}{N}\sum_{\mathbf{k}}J^{\alpha,e}_{\mathbf{k}}J^{\beta,e}_{\mathbf{k}}\left[\frac{n_f(E_{\mathbf{k},-})-n_f(E_{\mathbf{k}+\mathbf{q},-})}{\omega+E_{\mathbf{k},-}-E_{\mathbf{k}+\mathbf{q},-}+\mathrm{i}0^+}\right], \tag{15}$$

where $n_f(\epsilon)=1/[1+\exp(\epsilon/T)]$ is the Fermi-Dirac distribution function. Since we are specifically interested in the dc response ($\omega=0$), afterwards we drop ω from our calculations. In the local limit ($\mathbf{q}\to0$), one finds

$$\mathrm{Re}[\Delta\mathbb{K}_{\alpha\beta}(\mathbf{q}=0,T)]=-\sum_{\mathbf{k}}\frac{J^{\alpha,e}_{\mathbf{k}}J^{\beta,e}_{\mathbf{k}}}{4T\cosh^2(E_{\mathbf{k},-}/2T)}. \tag{16}$$

While the magnetic penetration depth is linked to the real component of the electromagnetic response tensor, we have [9]

$$\lambda^{\mathrm{loc}}_{\alpha\beta}(T)=\left[\frac{4\pi}{c}\mathrm{Re}[\mathbb{K}_{\alpha\beta}(\mathbf{q}=0,T)]\right]^{-\frac{1}{2}}. \tag{17}$$

In this context, we can thus formulate the magnetic penetration depth for a superconductor with an arbitrary Fermi surface as

$$\lambda^{\mathrm{loc}}_{\alpha\beta}(T)=\lambda_0\left[\delta_{\alpha\beta}-\sum_{\mathbf{k}}\frac{J^{\alpha,e}_{\mathbf{k}}J^{\beta,e}_{\mathbf{k}}}{4\mathbb{K}_0T}\cosh^{-2}\left(\frac{E_{\mathbf{k}}}{2T}\right)\right]^{-\frac{1}{2}}. \tag{18}$$

Hence, within the low-temperature regime, $T\ll T_C$, we can derive

$$\lambda_{\mathrm{loc}}(T)\approx\lambda_0\left[\delta_{\alpha\beta}+\sum_{\mathbf{k}}\frac{J^{\alpha,e}_{\mathbf{k}}J^{\beta,e}_{\mathbf{k}}}{8\mathbb{K}_0T}\cosh^{-2}\left(\frac{E_{\mathbf{k}}}{2T}\right)\right]. \tag{19}$$

However, for the nonlocal limit ($\mathbf{q}\neq0$), the electrons are reflected by the boundary either specularly or diffusively. In both regimes, the penetration depth is related to the superconducting properties of the material, such as its critical temperature and the density of superconducting carriers. It is also influenced by external factors such as temperature and the frequency of the incident electromagnetic waves.

For the *specular boundary condition*, the magnetic penetration depth is determined by [9]

$$\lambda_{\mathrm{spec}}(T)=\frac{2}{\pi}\int_0^{\infty}dq[q^2+\mathrm{Re}[\mathbb{K}(\mathbf{q},T)]]^{-1}, \tag{20}$$

where electromagnetic waves incident on the superconductor are reflected in a predictable and orderly manner, similar to the way light reflects off a mirror. This regime typically applies to smooth and clean surfaces of the superconductor. Moreover, the penetration depth refers to the depth at which the amplitude of the electromagnetic field decreases by a factor of $1/e$ (about 37%) compared to its value at the surface.

On the other hand, when considering a *diffusive boundary*, one can find [9]

$$\lambda_{\mathrm{diff}}(T)=\pi\left[\int_0^{\infty}dq\ln\left(1+\frac{4\pi}{c}\frac{\mathrm{Re}[\mathbb{K}(\mathbf{q},T)]}{q^2}\right)\right]^{-1}, \tag{21}$$

where the electromagnetic waves incident on the superconductor are scattered in various directions due to surface roughness, impurities, or defects present on the surface. The penetration depth refers to the average distance over which the electromagnetic field is attenuated inside the superconductor. This regime typically applies to rough or dirty surfaces.

We are also interested in the normalized superfluid density tensor, which can be expressed in terms of the magnetic penetration depth as [21]

$$\rho^s(T)=\left[\frac{\lambda(T)}{\lambda_0}\right]^{-2}. \tag{22}$$

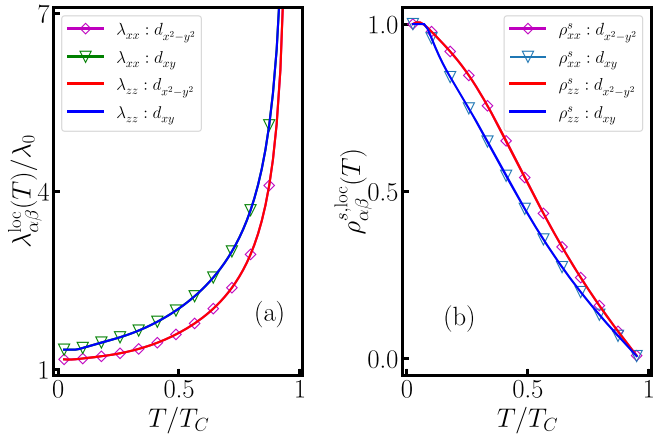

FIG. 2. Temperature dependence of (a) xx and zz components of the penetration depth, and (b) normalized superfluid density for possible $d_{x^2-y^2}$- and d_{xy}-wave pairings in $CeCoIn_5$ in the local limit ($\mathbf{q} \to 0$). Note: Here, the London penetration depth is normalized by $\lambda_0 = \sqrt{\frac{m_e c^2}{4\pi e^2 n_s}}$, with electron mass (charge) m_e (e), and superfluid of concentration n_s.

For the simplistic case, namely an s-wave superconductor with a spherical Fermi surface in the local limit, our approach yields

$$\rho^s(T) = 1 + 2\int d\varepsilon \frac{\partial n_f(E_{\mathbf{k}})}{\partial E_{\mathbf{k}}} = 1 - \frac{1}{2T}\int d\varepsilon \cosh^{-2}\left(\frac{\sqrt{\varepsilon^2+\Delta^2}}{2T}\right), \tag{23}$$

which is the familiar expression of superfluid density for isotropic s-wave pairing [6,53].

This approach establishes the connection between the complex microscopic state for the most general superconductor and the macroscopic penetration depth which can be experimentally measured. Thus it can reveal the complex nature of the superconducting gap and its pairing symmetry. In particular, an exponential or temperature-independent behavior suggests a conventional s-wave superconducting gap (nodeless). Conversely, at low temperatures, for unconventional pairing the penetration depth can be approximated by a power-law-type behavior, $\lambda(T) \propto T^n$, which can imply the existence of nodal superconductivity. The type of nodes in the system determines the value of the power exponent. A linear to quadratic temperature dependence analogizes the presence of line nodes or point nodes in the superconducting gap.

IV. RESULTS OF PENETRATION DEPTH FOR $CeCoIn_5$

In this section, we delve into the outcomes of our investigation into the penetration depth of $CeCoIn_5$, with a specific focus on symmetry-related aspects. It is important to note that due to the in-plane C_{4v} rotational symmetry, an expected equivalence arises between the xx and yy components of the penetration depth and superfluid density tensors. However, we should underscore that no such guarantee exists for the zz component. Here, in addition to the primary candidate pairing, $d_{x^2-y^2}$, $\Delta_0(T)(\cos k_x - \cos k_y)$, we also investigate d_{xy} pairing, $\Delta_0(T)\sin k_x \sin k_y$. In the strong-coupling limit, the temperature dependence of the superconducting order parameter is assumed to be of the form $\Delta_0(T) = \Delta_0 \tanh[1.76\sqrt{T_C/T - 1}]$, with Δ_0 as the amplitude of the pairing.

In the local limit (see Fig. 2), a theoretical prediction is fulfilled: All components of the penetration depth and superfluid density tensors (xx, yy, and zz) converge to identical values. Notably, within this limit, we made a significant observation that the penetration depth of d_{xy}-wave pairing surpasses that of $d_{x^2-y^2}$-wave pairing. Inversely, the superfluid density of $d_{x^2-y^2}$ dominates over that of d_{xy}. Moving into the nonlocal limit, Fig. 3(a) investigates the specular scattering regime, revealing fascinating insights into the penetration depth's behavior. Particularly at higher temperatures, we observed a remarkable convergence in the zz-component values for both d-wave pairings, indicating a trend toward parity. Notably, these zz-component values are significantly greater than those

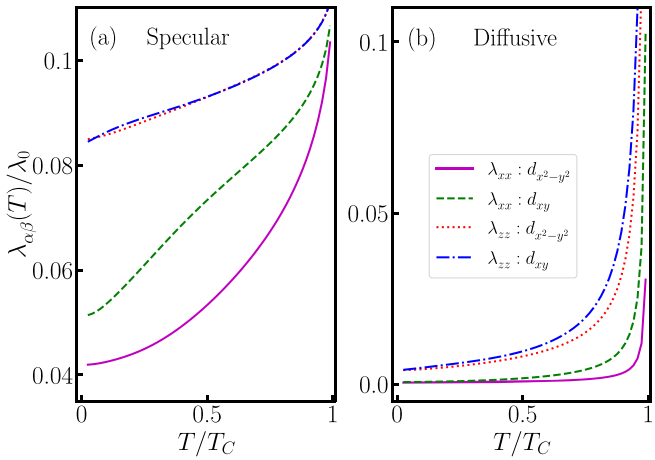

FIG. 3. The xx and zz components of $\lambda(T)$ for $CeCoIn_5$ in (a) specular and (b) diffusive regimes, considering possible $d_{x^2-y^2}$- and d_{xy}-wave pairings. Similar to Fig. 2, the London penetration depth is normalized here.

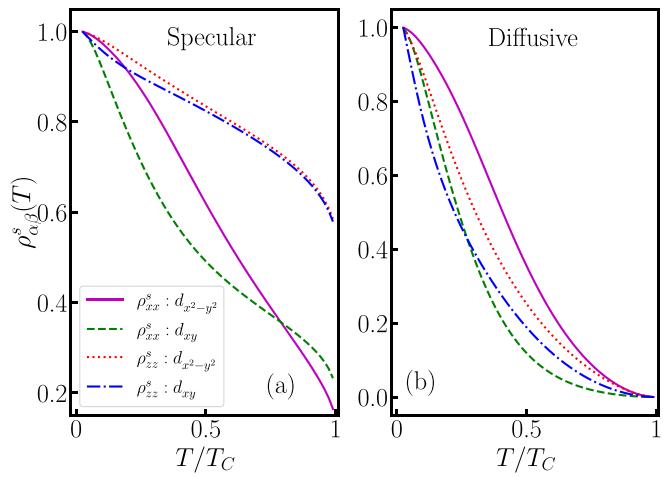

FIG. 4. The spatial components of the normalized superfluid density tensor of possible $d_{x^2-y^2}$ and d_{xy} Cooper pairings in $CeCoIn_5$ for nonlocal (a) specular and (b) diffusive regimes.

TABLE I. The values of the exponent in the power-law relationship between the London penetration depth versus temperature at the low-temperature limit ($T/T_C < 1/3$).

Pairing	Component	Local	Specular	Diffusive
$d_{x^2-y^2}$	xx	1.88	1.89	2.07
	zz	1.88	1.17	1.56
d_{xy}	xx	1.17	1.15	1.90
	zz	1.17	0.61	1.20

recorded for the xx and yy components. Furthermore, we observe a striking dominance of the penetration depth for d_{xy}-wave pairing over its $d_{x^2-y^2}$-wave counterpart in the xx and yy components. In the diffusive regime, as shown in Fig. 3(b), we have uncovered a distinct behavior within the penetration depth characteristics. In contrast to the specular regime, the zz component exhibits a clear preference for d_{xy}-wave pairing over $d_{x^2-y^2}$-wave pairing. This pattern is mirrored in the xx components, further accentuating the dominance of d_{xy}-wave pairing in this particular scattering regime.

Furthermore, Fig. 4 represents the temperature dependence of superfluid density in the nonlocal limit. In the specular regime, this quantity strongly depends on the symmetry of the superconducting gap. In addition, for every specific type of order parameter, an obvious difference is apparent between the xx and zz components of the superfluid density, especially at higher temperatures. However, in the diffusive regime, there are lesser differences among the components of the superfluid density for both $d_{x^2-y^2}$ and d_{xy} pairings.

At the end, Table I provides the exponent that characterizes the power-law temperature dependence of the London penetration depth in the low-temperature regime ($T/T_C < 1/3$). Both the in-plane (xx) and out-of-plane (zz) components of $\lambda(T)$ are offered for $d_{x^2-y^2}$- and d_{xy}-wave pairings, characterized by both London (local) and Pippard (nonlocal) properties. These findings reveal a departure from the behavior of $\lambda(T) \sim T$ towards $\lambda(T) \sim T^2$ at low temperatures. This deviation is in line with the presence of line nodes [or point nodes in two dimensions (2D)] in the superconducting pairing symmetry. In the case of experimental observations in $CeCoIn_5$, it becomes apparent that λ_{xx} undergoes a crossover, transitioning from a behavior proportional to T to one proportional to T^2 [48,54–56]. Furthermore, the well-established Kosztin-Leggett prediction suggests that λ_{zz} behaves as $\sim T$ [20]. Our results confirm the dominant f nonlocal behavior in the superconducting state and they align more consistently with prior efforts in the $d_{x^2-y^2}$ pairing in the specular nonlocal regime. Additionally, they concur with the thermal-conductivity measurements performed in the presence of an in-plane applied magnetic field, which demonstrates fourfold symmetry. They also pinpoint the nodes situated at the $(\pm\pi, \pm\pi)$ positions within the Brillouin zone [39].

V. SUMMARY

We present a microscopic formulation of the London (magnetic) penetration depth, specifically designed for heavy-fermion superconductors, with a focus on $CeCoIn_5$, a representative system known for its suggested d-wave pairings. Our formulation establishes a crucial link between the intricate microscopic superconducting state and the experimentally observable macroscopic properties in these materials. We demonstrate that the temperature-dependent behavior of the penetration depth is influenced by both the superconducting gap structure and the complex Fermi-surface topology. Particularly, our study provides evidence that $CeCoIn_5$ exhibits London-type superconductivity, where the penetration depth significantly exceeds the coherency length [7]. Furthermore, in the nonlocal limit, the temperature-dependent behavior of the London penetration depth suggests that the prevailing superconducting pairing mechanism for $CeCoIn_5$ is the nodal $d_{x^2-y^2}$ symmetry. These features are closely aligned with thermal conductivity measurements [39], and magnetic force microscopy results [48]. This versatile approach is applicable to a wide range of physical systems, making it valuable for exploring superconducting behaviors in various materials.

ACKNOWLEDGMENTS

We acknowledge helpful discussions with Geunyong Kim, Jinyoung Youn, and M. N. Najafi. We are grateful to Yunkyu Bang and Ki-Seok Kim for their insightful comments. M.B. thanks H. Yavari for valuable conversations. A.A. acknowledges the financial support from the German Research Foundation within the bilateral NSFC-DFG Project No. ER 463/14-1.

[1] J. G. Bednorz and K. A. Müller, Possible high T_c superconductivity in the Ba − La − Cu − O system, Z. Phys. B: Condens. Matter **64**, 189 (1986).

[2] P. Monthoux, D. Pines, and G. G. Lonzarich, Superconductivity without phonons, Nature (London) **450**, 1177 (2007).

[3] M. R. Norman, The challenge of unconventional superconductivity, Science **332**, 196 (2011).

[4] D. J. Scalapino, A common thread: The pairing interaction for unconventional superconductors, Rev. Mod. Phys. **84**, 1383 (2012).

[5] V. Mineev and K. Samokhin, *Introduction to Unconventional Superconductivity* (Gordon and Breach, London, 1999).

[6] R. Prozorov and R. W. Giannetta, Magnetic penetration depth in unconventional superconductors, Supercond. Sci. Technol. **19**, R41 (2006).

[7] A. Abrikosov, L. Gorkov, and I. Dzyaloshinski, *Methods of Quantum Field Theory in Statistical Physics* (Dover, New York, 1975).

[8] G. Eliashberg, G. Klimovitch, and A. Rylyakov, On the temperature dependence of the London penetration depth in a superconductor, J. Supercond. **4**, 393 (1991).

[9] M. Tinkham, *Introduction to Superconductivity*, 2nd ed. (Dover, New York, 2004).

[10] I. Bonalde, R. L. Ribeiro, W. Brämer-Escamilla, G. Mu, and H. H. Wen, Possible two-gap behavior in noncentrosymmetric superconductor $Mg_{10}Ir_{19}B_{16}$: A penetration depth study, Phys. Rev. B **79**, 052506 (2009).

[11] V. G. Kogan and R. Prozorov, Temperature dependence of London penetration depth anisotropy in superconductors with anisotropic order parameters, Phys. Rev. B **103**, 054502 (2021).

[12] W. Barford and J. Gunn, The theory of the measurement of the London penetration depth in uniaxial type II superconductors by muon spin rotation, Phys. C: Supercond. **156**, 515 (1988).

[13] B. Pümpin, H. Keller, W. Kündig, W. Odermatt, I. M. Savić, J. W. Schneider, H. Simmler, P. Zimmermann, E. Kaldis, S. Rusiecki, Y. Maeno, and C. Rossel, Muon-spin-rotation measurements of the London penetration depths in $YBa_2Cu_3O_{6.97}$, Phys. Rev. B **42**, 8019 (1990).

[14] M. Roseman and P. Grütter, Estimating the magnetic penetration depth using constant-height magnetic force microscopy images of vortices, New J. Phys. **3**, 24 (2001).

[15] R. Khasanov, I. L. Landau, C. Baines, F. La Mattina, A. Maisuradze, K. Togano, and H. Keller, Muon-spin-rotation measurements of the penetration depth in Li_2Pd_3B, Phys. Rev. B **73**, 214528 (2006).

[16] J. Kim, L. Civale, E. Nazaretski, N. Haberkorn, F. Ronning, A. S. Sefat, T. Tajima, B. H. Moeckly, J. D. Thompson, and R. Movshovich, Direct measurement of the magnetic penetration depth by magnetic force microscopy, Supercond. Sci. Technol. **25**, 112001 (2012).

[17] M. Eltschka, B. Jaeck, M. Assig, O. Kondrashov, M. Skvortsov, M. Etzkorn, C. Ast, and K. Kern, Superconducting scanning tunneling microscopy tips in a magnetic field: Geometry-controlled order of the phase transition, Appl. Phys. Lett. **107**, 122601 (2015).

[18] M. W. Coffey, Analyzing mutual inductance measurements to determine the London penetration depth, J. Appl. Phys. **87**, 4344 (2000).

[19] R. Harris, J. Johansson, A. J. Berkley, M. W. Johnson, T. Lanting, S. Han, P. Bunyk, E. Ladizinsky, T. Oh, I. Perminov, E. Tolkacheva, S. Uchaikin, E. M. Chapple, C. Enderud, C. Rich, M. Thom, J. Wang, B. Wilson, and G. Rose, Experimental demonstration of a robust and scalable flux qubit, Phys. Rev. B **81**, 134510 (2010).

[20] I. Kosztin and A. J. Leggett, Nonlocal effects on the magnetic penetration depth in d-wave superconductors, Phys. Rev. Lett. **79**, 135 (1997).

[21] N. Hayashi, K. Wakabayashi, P. A. Frigeri, and M. Sigrist, Temperature dependence of the superfluid density in a noncentrosymmetric superconductor, Phys. Rev. B **73**, 024504 (2006).

[22] J. Chen, L. Jiao, J. L. Zhang, Y. Chen, L. Yang, M. Nicklas, F. Steglich, and H. Q. Yuan, Evidence for two-gap superconductivity in the non-centrosymmetric compound $LaNiC_2$, New J. Phys. **15**, 053005 (2013).

[23] F. O. von Rohr, J.-C. Orain, R. Khasanov, C. Witteveen, Z. Shermadini, A. Nikitin, J. Chang, A. R. Wieteska, A. N. Pasupathy, M. Z. Hasan, A. Amato, H. Luetkens, Y. J. Uemura, and Z. Guguchia, Unconventional scaling of the superfluid density with the critical temperature in transition metal dichalcogenides, Sci. Adv. **5**, eaav8465 (2019).

[24] T. C. Wu, H. K. Pal, P. Hosur, and M. S. Foster, Power-law temperature dependence of the penetration depth in a topological superconductor due to surface states, Phys. Rev. Lett. **124**, 067001 (2020).

[25] D. Collomb, S. J. Bending, A. E. Koshelev, M. P. Smylie, L. Farrar, J.-K. Bao, D. Y. Chung, M. G. Kanatzidis, W.-K. Kwok, and U. Welp, Observing the suppression of superconductivity in $RbEuFe_4As_4$ by correlated magnetic fluctuations, Phys. Rev. Lett. **126**, 157001 (2021).

[26] S. Dzhumanov, U. Turmanova, and U. Kurbanov, Two distinctive temperature dependences of the london penetration depth in high-T_c cuprate superconductors as support for the theory of Bose-liquid superconductivity, Phys. Lett. A **452**, 128447 (2022).

[27] J. D. Fletcher, A. Carrington, P. Diener, P. Rodière, J. P. Brison, R. Prozorov, T. Olheiser, and R. W. Giannetta, Penetration depth study of superconducting gap structure of $2H$-$NbSe_2$, Phys. Rev. Lett. **98**, 057003 (2007).

[28] H. Kim, M. A. Tanatar, R. Flint, C. Petrovic, R. Hu, B. D. White, I. K. Lum, M. B. Maple, and R. Prozorov, Nodal to nodeless superconducting energy-gap structure change concomitant with Fermi-surface reconstruction in the heavy-fermion compound $CeCoIn_5$, Phys. Rev. Lett. **114**, 027003 (2015).

[29] F. Steglich, J. Aarts, C. D. Bredl, W. Lieke, D. Meschede, W. Franz, and H. Schäfer, Superconductivity in the presence of strong Pauli paramagnetism: $CeCu_2Si_2$, Phys. Rev. Lett. **43**, 1892 (1979).

[30] A. Hewson, *The Kondo Problem to Heavy Fermions*, Cambridge Studies in Magnetism (Cambridge University Press, Cambridge, UK, 1993).

[31] C. Pfleiderer, Superconducting phases of f-electron compounds, Rev. Mod. Phys. **81**, 1551 (2009).

[32] C. Petrovic, P. G. Pagliuso, M. F. Hundley, R. Movshovich, J. L. Sarrao, J. D. Thompson, Z. Fisk, and P. Monthoux, Heavy-fermion superconductivity in $CeCoIn_5$ at 2.3 K, J. Phys.: Condens. Matter **13**, L337 (2001).

[33] A. Bianchi, R. Movshovich, I. Vekhter, P. G. Pagliuso, and J. L. Sarrao, Avoided antiferromagnetic order and quantum critical point in $CeCoIn_5$, Phys. Rev. Lett. **91**, 257001 (2003).

[34] J. Paglione, M. A. Tanatar, D. G. Hawthorn, E. Boaknin, R. W. Hill, F. Ronning, M. Sutherland, L. Taillefer, C. Petrovic, and P. C. Canfield, Field-induced quantum critical point in $CeCoIn_5$, Phys. Rev. Lett. **91**, 246405 (2003).

[35] J. L. Sarrao and J. D. Thompson, Superconductivity in cerium- and plutonium-based '115' materials, J. Phys. Soc. Jpn. **76**, 051013 (2007).

[36] J. D. Thompson and Z. Fisk, Progress in heavy-fermion superconductivity: Ce115 and related materials, J. Phys. Soc. Jpn. **81**, 011002 (2012).

[37] A. Gyenis, B. E. Feldman, M. T. Randeria, G. A. Peterson, E. D. Bauer, P. Aynajian, and A. Yazdani, Visualizing heavy fermion confinement and Pauli-limited superconductivity in layered $CeCoIn_5$, Nat. Commun. **9**, 549 (2018).

[38] V. A. Sidorov, M. Nicklas, P. G. Pagliuso, J. L. Sarrao, Y. Bang, A. V. Balatsky, and J. D. Thompson, Superconductivity and quantum criticality in $CeCoIn_5$, Phys. Rev. Lett. **89**, 157004 (2002).

[39] K. Izawa, H. Yamaguchi, Y. Matsuda, H. Shishido, R. Settai, and Y. Onuki, Angular position of nodes in the superconducting

gap of quasi-2D heavy-fermion superconductor $CeCoIn_5$, Phys. Rev. Lett. **87**, 057002 (2001).

[40] W. K. Park, J. L. Sarrao, J. D. Thompson, and L. H. Greene, Andreev reflection in heavy-fermion superconductors and order parameter symmetry in $CeCoIn_5$, Phys. Rev. Lett. **100**, 177001 (2008).

[41] C. Stock, C. Broholm, J. Hudis, H. J. Kang, and C. Petrovic, Spin resonance in the d-wave superconductor $CeCoIn_5$, Phys. Rev. Lett. **100**, 087001 (2008).

[42] I. Eremin, G. Zwicknagl, P. Thalmeier, and P. Fulde, Feedback spin resonance in superconducting $CeCu_2Si_2$ and $CeCoIn_5$, Phys. Rev. Lett. **101**, 187001 (2008).

[43] A. Akbari and P. Thalmeier, Field-induced spin exciton doublet splitting in $d_{x^2-y^2}$-wave $CeMIn_5$ (M = Rh, Ir, Co) heavy-electron superconductors, Phys. Rev. B **86**, 134516 (2012).

[44] K. An, T. Sakakibara, R. Settai, Y. Onuki, M. Hiragi, M. Ichioka, and K. Machida, Sign reversal of field-angle resolved heat capacity oscillations in a heavy fermion superconductor $CeCoIn_5$ and $d_{x^2-y^2}$ pairing symmetry, Phys. Rev. Lett. **104**, 037002 (2010).

[45] A. Akbari, P. Thalmeier, and I. Eremin, Quasiparticle interference in the heavy-fermion superconductor $CeCoIn_5$, Phys. Rev. B **84**, 134505 (2011).

[46] M. Allan, F. Massee, D. Morr, J. Dyke, A. Rost, A. Mackenzie, C. Petrovic, and J. Davis, Imaging Cooper pairing of heavy fermions in $CeCoIn_5$, Nat. Phys. **9**, 468 (2013).

[47] B. Zhou, S. Misra, E. Neto, P. Aynajian, R. Baumbach, J. Thompson, E. Bauer, and A. Yazdani, Visualizing nodal heavy fermion superconductivity in $CeCoIn_5$, Nat. Phys. **9**, 474 (2013).

[48] D. Wulferding, G. Kim, H. Kim, I. Yang, E. D. Bauer, F. Ronning, R. Movshovich, and J. Kim, Local characterization of a heavy-fermion superconductor via sub-Kelvin magnetic force microscopy, Appl. Phys. Lett. **117**, 252601 (2020).

[49] K. Tanaka, H. Ikeda, Y. Nisikawa, and K. Yamada, Theory of superconductivity in $CeMIn_5$ (M = Co, Rh, Ir) on the basis of the three dimensional periodic Anderson model, J. Phys. Soc. Jpn. **75**, 024713 (2006).

[50] P. Coleman, *Introduction to Many-Body Physics* (Cambridge University Press, Cambridge, UK, 2015).

[51] H. Kontani, J. Goryo, and D. S. Hirashima, Intrinsic spin Hall effect in the s-wave superconducting state: Analysis of the Rashba model, Phys. Rev. Lett. **102**, 086602 (2009).

[52] M. Biderang and H. Yavari, Spin Hall conductivity in the impure two-dimensional Rashba s-wave superconductor, Phys. C: Supercond. Appl. **525-526**, 100 (2016).

[53] I. Bonalde, W. Brämer-Escamilla, and E. Bauer, Evidence for line nodes in the superconducting energy gap of noncentrosymmetric $CePt_3Si$ from magnetic penetration depth measurements, Phys. Rev. Lett. **94**, 207002 (2005).

[54] E. E. M. Chia, D. J. Van Harlingen, M. B. Salamon, B. D. Yanoff, I. Bonalde, and J. L. Sarrao, Nonlocality and strong coupling in the heavy fermion superconductor $CeCoIn_5$: A penetration depth study, Phys. Rev. B **67**, 014527 (2003).

[55] S. Özcan, D. M. Broun, B. Morgan, R. K. W. Haselwimmer, J. L. Sarrao, S. Kamal, C. P. Bidinosti, P. J. Turner, M. Raudsepp, and J. R. Waldram, London penetration depth measurements of the heavy-fermion superconductor $CeCoIn_5$ near a magnetic quantum critical point, Europhys. Lett. **62**, 412 (2003).

[56] K. Hashimoto, Y. Mizukami, R. Katsumata, H. Shishido, M. Yamashita, H. Ikeda, Y. Matsuda, J. A. Schlueter, J. D. Fletcher, A. Carrington, D. Gnida, D. Kaczorowski, and T. Shibauchi, Anomalous superfluid density in quantum critical superconductors, Proc. Natl. Acad. Sci. USA **110**, 3293 (2013).